Mekanika: Majalah Ilmiah Mekanika

An MR Damper Parametric Model with luz(...) Projection Function and Its Application in an Open-loop Force Tracking Control System

Raymundus Lullus Lambang Govinda Hidayat[1*], Fitrian Imaduddin[2,3], Budi Santoso[2], Irianto[4], Azma Putra[5], Ubaidillah[2]

1 Doctoral Candidate in Department of Mechanical Engineering, Sebelas Maret University, Surakarta, Indonesia
2 Professor in Department of Mechanical Engineering, Sebelas Maret University, Surakarta, Indonesia
3 Department of Mechanical Engineering, Islamic University of Madinah, Madinah, Saudi Arabia
4 Department General Education, Faculty of Resilience, Rabdan Academy, Abu Dhabi, United Arab Emirates
5 School of Civil and Mechanical Engineering, Curtin University, Bentley, Australia

*Corresponding Author's email address: lulus_l@staff.uns.ac.id

Abstract
This research discusses a parametric model with a luz(...) projection function for an outer bypass Magnetorheological (MR) damper with a meandering type valve and its application in an open-loop force tracking control system. This parametric model with the luz(…) projection function has been developed previously. The MR damper force can be controlled with open-loop force as a standard control strategy. Research on the performance of the MR damper model in open-loop control systems usually uses non-parametric models. Thus, the novelty of this research is that it uses a parametric model, i.e., the model of the luz(...) projection function as the model of the outer bypass MR damper with a meandering type valve. The proposed open-loop control system uses an inverse model that produces an electric current according to the desired force. The force tracking control scheme was realized with computer simulations using a state space approach. These simulation results show that the model with the luz(…) projection function can efficiently and accurately track the desired force in an open-loop force-tracking control system. The desired force is sinusoidal, square, and sawtooth waveform. Relative Error (RE) of 0.000, 0.0123, and 0.0563, respectively, are achieved.

1 Introduction

A Magnetorheological (MR) damper is an intelligent tool used in a vibration mitigation system, such as in a vehicle or automotive suspension and building seismic protection [1-3]. The vibration mitigation system uses a control system that consists of springs and shock absorbers according to the functionality point of view. Springs can be leaf springs, coil springs, air springs, and shock absorbers can be viscous dampers or electrorheological or magnetorheological (MR) dampers. Today, magnetorheological (MR) damper has been extensively studied and developed in automotive manufacturing because of its simple structure, wide damping force range, and quick responses.

Hidayat et al.

In the design phase of the vehicle suspension control system, there is a numerical simulation to investigate the performance of the MR damper [4]. The numerical simulation uses an MR damper model. However, MR damper models are challenging to obtain due to their highly nonlinear nature. This research is also motivated by a new MR damper development. Indonesian and Malaysian researchers have developed a prototype outer bypass MR damper with a meandering-type valve [5]. Previous research has produced a non-parametric outer bypass MR damper model with a meandering type valve [6]. The research gap is that a parametric model for outer bypass MR dampers with meandering valves has not been developed yet.

The MR damper models that have been developed are the Bouc-Wen model [7], the nonlinear viscous model [8], and the Bingham model [9]. These models are parametric. They predict the damping force of an MR damper. However, these models are complicated to use in a control system (open or closed loop) to achieve high force tracking control performance. Also, these models make it difficult for us to realize a control system because the parameters of these models are determined experimentally, and the operation condition changes. This research proposes a model with a luz(...) projection function for an outer bypass MR damper with a meandering type valve that can be easily integrated into a force-tracking control system. The luz(…) projection function as it is explained in [10,11].

This research contributes to the development of an open-loop force tracking control system consisting of an MR damper model with the luz(...) projection function and its inverse model. The accuracy of this open loop force tracking control system is evaluated using the desired force of sinusoidal, square, and sawtooth waves. The open-loop force tracking control system uses an inverse model that produces an electric current from the desired force. The performance of the luz(…) projection function model-based open loop force tracking control system is evaluated numerically with computer simulations. The simulation is performed using a state-space approach. As a comparison, an open loop force tracking control system with the Bingham model and the inverse Bingham model is developed and evaluated. The Bingham model is only considered because it cannot describe the hysteresis as the Bouc-Wen model, similar to the luz(…) projection function model. The viscous model is a piecewise function model, so its inverse model is challenging.

The rest of this paper is organized as follows. Section 2 briefly discusses magnetorheological fluids and magnetorheological dampers, the construction and working principles of outer bypass MR dampers with meandering type valves, and the damper characterization. Section 3 explains the existing MR damper models and the model with the luz(…) projection function. Section 4 explains the force tracking control system. Section 5 describes the results of this research, and Section 6 presents conclusions and future research based on this research.

2 Magnetorheological Fluid and Magnetorheological Fluid Damper

2.1 MR fluid

The inventor of Magnetorheological Fluid (MRF) was Jacob Rabinow from the United States (US) National Bureau of Standards in the late 1940s [12]. This fluid is a micron-sized magnetizable particle solution in a carrier liquid [13]. MRF contains 20-40% by volume of soft iron particles (e.g., carbonyl iron). These particles are suspended in mineral oil, synthetic oil, water, or glycol. An additive, the same kind as commercial lubricants, is usually added to MRF to inhibit settling due to gravity, inhibit clumping, and increase lubrication capabilities, thereby reducing wear.

MRF is a free-flowing liquid similar to motor lubricant oil. However, if a magnetic field is applied, the iron particles will experience a dipole moment, which is aligned with the external magnetic field flux, causing the particles to form linear chains parallel to the flux, as shown in Figure 1. This phenomenon can solidify dissolved particles (suspended iron particles) and limit the movement of the fluid. As a result, fatigue and stress from the fluid grow. The stress change rate is proportional to the magnitude of the applied magnetic field and occurs in a millisecond.
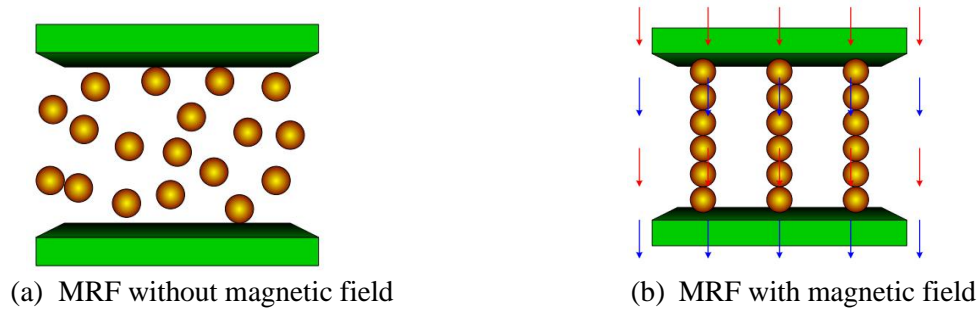
Hidayat et al.

(a) MRF without magnetic field   (b) MRF with magnetic field

Figure 1. Working principle of Magnetorheological Fluid (MRF)

The rheological property (viscosity) of magnetorheological fluids depends on the strength of the magnetic field. The viscous properties of MRF differ in the pre-yield and post-yield regions. MRF exhibits visco-elastic behavior in the pre-yield region, and in the post-yield region, MRF behaves like a Newtonian viscous fluid [14].

2.2 Outer bypass MR damper with meandering type valve

The MR damper discussed in this study is an outer bypass MR damper with a meandering type valve, as shown in Figure 2 [15]. Figure 2 shows that the MR damper consists of two sections, i.e., the column section and the bypass section. The column section consists of the cylinder, piston, and piston rod. The bypass section consists of a channel (conduit) and a valve. When the piston moves in the cylinder, the MR fluid in the front chamber of the piston will be pressed and flow through the bypass channel to the valve. The valve resists MRF flow. Variations in the resistance of fluid flow produced in the valve are caused by variations in the fatigue/shear stress of the MRF, which is controlled by the magnetic field. Variations in the fatigue/shear stress of the MRF result in variations in the damping force of the MR damper.

The construction of an outer bypass MR damper with a meandering type valve is unlike the inner bypass MR damper with the valve at the piston. The outer bypass MR damper valve is installed outside the cylinder. Even though the total size (length, width, and height) of the outer bypass MR damper is larger than the inner bypass MR damper, placing the valve outside the cylinder provides the benefit of being able to choose the valve and free-installation because the diameter and length of the cylinder do not limit the valve size. Apart from this, we can obtain a large force damping range to vary the damping force. Another benefit is easy installation and modification because the valve can be replaced without rearranging the MR damper cylinder [15].

The MR valve contains an electromagnetic circuit where the magnetic flux is designed to pass through the MR fluid channel. The magnetic field perpendicularly passing through the MR fluid flows changes the fluid behavior from a Newtonian free-flow fluid to a non-Newtonian one. The magnetic flux density is regulated in such a way as to regulate the fluid fatigue stress, which produces a pressure difference between the valve inlet and outlet and then controls the fluid flow. The intersection between the magnetic flux and the fluid is critical because pressure drops only occur in this area. The area of this intersection is called the effective area. The arrangement and configuration of the channels in the valve determine the effective area.

A meandering type valve is a valve with an annular and radial channel arrangement. Meandering-type valves can produce large pressure drops because they use a combination of annular and radial channels to increase effective area. The meandering valve allows more MRF to flow through this small valve to control the wide range of pressure drops. With this valve performance, a wide range of damping force can be achieved with a small MR damper size [16]. A detailed description of meandering-type valves is given in [15,17,18]. Research by Shimadzu [19] discusses the latest outer bypass MR damper application with meandering-type valves.
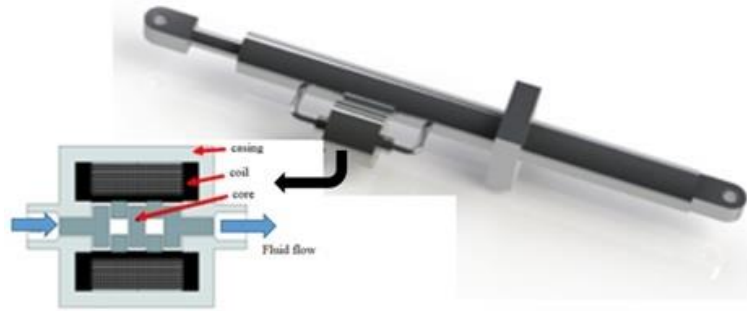
Hidayat et al.

Figure 2. Schematic of outer bypass MR damper with meandering type valve [15]

2.3 Characteristics of outer bypass MR Damper with meandering type valve

The characteristics of the outer bypass MR damper with a meandering type valve were obtained in previous experimental tests [15]. The experimental setup is shown in Figure 3. Figure 3 (a) shows the schematic of the MR damper prototype test, and Figure 3b shows the experimental setup. Experiments use a dynamic fatigue testing machine, i.e., servo-hydraulic fatigue and endurance tester [20]. This machine applies sinusoidal excitation. A load cell measures the damping force produced by the damper. A displacement sensor measures the MR damper piston position. The maximum load capacity of the dynamic fatigue testing machine is 1 ton (1000 kg), and the maximum speed is 1 m/s. The MR damper had a maximum stroke of 55 mm [15]. This experiment maintained the stroke at 40 mm (amplitude 20 mm). The electric current input is 0 to 1.0 amperes with intervals of 0.1 amperes. This current is fed to the electromagnet circuit coil inside the MR damper valve. This input current is measured by using a DC clamp current meter. To ensure the consistency of the recorded data, 25 measurements were carried out, with each recorded data containing 25 sinusoidal displacement cycles.

A data acquisition system is used to record the force response and displacement of the MR damper. The data acquisition system has four analog channel inputs. The sinusoidal displacement from the computer becomes the input for the digital servo-controller that controls the hydraulic motion of this testing machine. The experiment was repeated to vary the current fed to the MR damper from 0 to 1.0 amperes with intervals of 0.1 amperes. MR damper piston displacement is measured with a Linear Variable Differential Transformer (LVDT) position sensor. The damping force is measured with a load cell. The LVDT signal and the signal from the load cell are then fed to the computer. These two signals are the recorded MR damper response (the data). The piston speed is obtained from the derivative of the position signal.
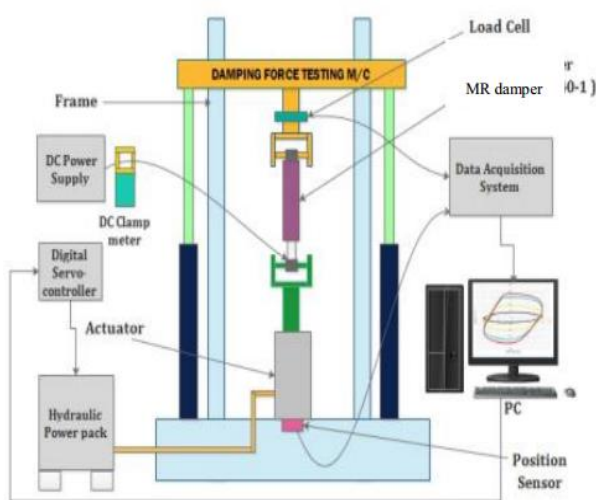
Figure 3. Experimental setup: (a) Experimental schematic, and (b) Experimental apparatus [15].
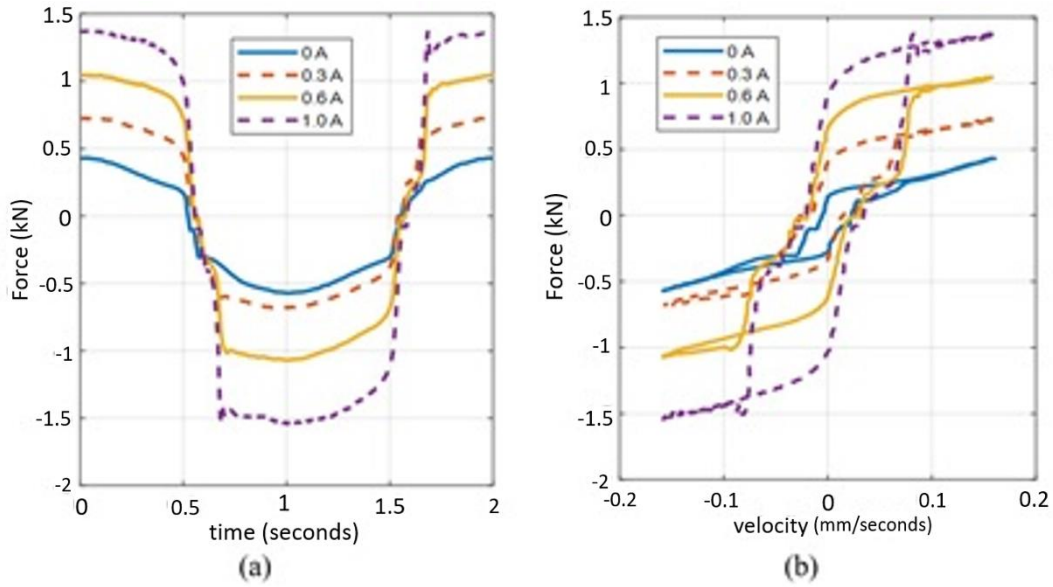
Hidayat et al.

Figure 4. Experimental results of the outer bypass MR damper prototype with a meandering type valve with current variations: (a) Damping force vs. time, and (b) Damping force vs. velocity [21].

Characterization of the outer bypass MR damper with a meandering type valve has been carried out experimentally [15]. Figure 4 shows the damper force vs. time graph and damper force vs. piston speed, respectively. If the electric current input is increased, the damping force increases because the pressure drops inside the valve increases. The damping force increases by 0.88 kN on average for every 0.3 ampere increase in electric current. The maximum damping force is 1.3 kN at 0.9 amperes. Figure 4 (b) shows the hysteresis properties as a loop graph consisting of 2 different curves, i.e., the upper and lower curves.

The upper curve and lower curve in the hysteresis loop is a damping force graph consisting of damping force due to pre-yield and post-yield fluid viscosity. In the pre-yield region, the viscosity of the MR fluid can be controlled by the magnetic flux in the valve. The magnetic flux is controlled by the current of the coil of the valve's electromagnetic circuit.

3 Damper Force Model

3.1 Bingham model

Stanway et al. [22] proposed the Bingham model to characterize the damping force of an Electrorheological (ER) damper. This model consists of a Coulomb friction element and a viscous dashpot, as shown schematically in Figure 5. The damping force of the MR damper produced by the Bingham model is shown in Equation 1 [9].

$$F_{damper} = f_c \, \text{sign}(U) + c_0 \cdot U + f_0 \tag{1}$$

c_0 is the damping coefficient, f_c is the friction force as a function of the fatigue stress of the MRF. U is the velocity of the MR damper piston. The Bingham model damper force graph vs. time and piston speed is shown in Figure 6. This model cannot explain the hysteresis characteristics of the MR damper.
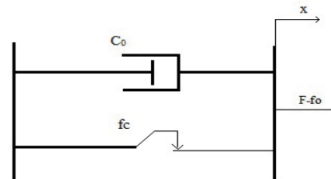

Figure 5. MR damper Bingham model (rheological structure of Bingham model [23])

Hidayat et al.

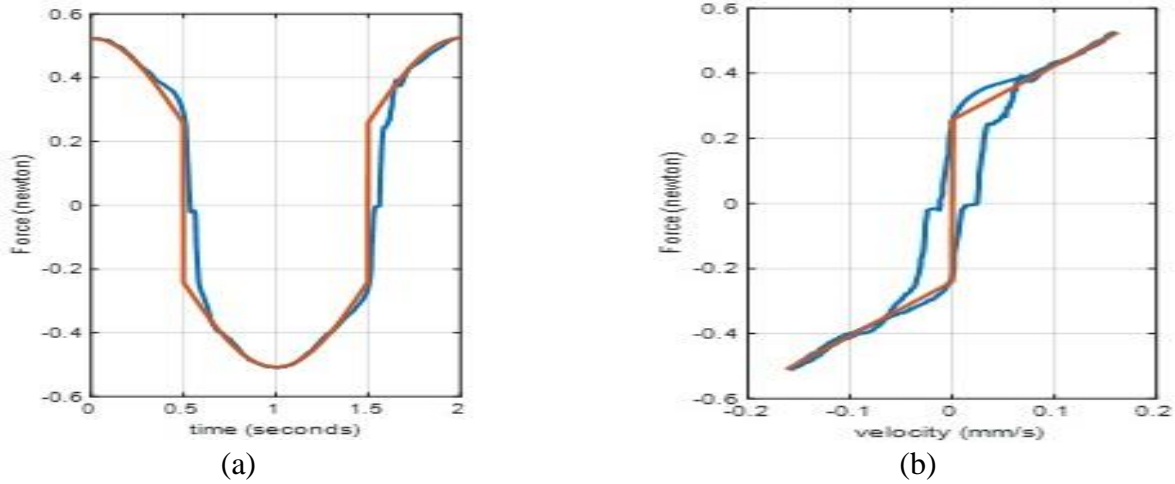(a)   (b)

Figure 6. Bingham model damper force graphs: (a) Damper force vs time, and (b) Damper force vs speed
(graphs generated from Matlab scripts)

Figure 6 (a) shows the Bingham model damper force vs. time (seconds) graph, and Figure 6 (b) shows the Bingham model damper force vs. piston speed (cm/s) graph. The model parameters F_c, c_0, and f_0 were obtained by applying the Particle Swarm Optimization (PSO) procedure [23] using experimental data of a prototype outer bypass MR damper with a meandering type valve. PSO optimization produces: $F_c = 0.2489$; $c_0 = 1.6589$; $f_0 = 0.0080$. The Relative Error (RE) value is determined in Equation 2.

$$RE = \frac{abs(F^{exp} - F^{model})}{abs(F^{exp})}$$ (2)

The RE value of the model with the above parameters is 0.094124.

3.2 Luz(…) projection function

A piecewise linear function is a function whose argument in an interval is divided into smaller intervals so that the function in each interval is linear. The projection function of a piecewise linear function is an analytic form of a piecewise linear function that applies to the argument in all intervals of the function. A projection function is a function that maps a piecewise linear function. Examples of a piecewise linear function and a projection function for the piecewise linear function are presented in Equations 3-4.

- Piecewise linear function:
$$y = \begin{cases} -x & \text{if } x \leq 0 \\ x & \text{if } x > 0 \end{cases}$$ (3a)
The projection function of the above piecewise linear function is:
$$y = x \cdot \text{sign}(x)$$ (3b)
Where:
$$\text{sign}(x) = \begin{cases} -1 & \text{if } x < 0 \\ 0 & \text{if } x = 0 \\ 1 & \text{if } x > 0 \end{cases}$$ (3c)
- Piecewise linear function:
$$y = \begin{cases} 0 & \text{if } x < 0 \\ x & \text{if } x \geq 0 \end{cases}$$ (4a)
The projection function of the above piecewise linear function is [10,11]:
$$y = diod(x) = \frac{x + |x|}{2} = x \cdot \left(\frac{1 + \text{sgn}(x)}{2}\right)$$ (4b)
Equations 3 (b), $y = x.\text{sgn}(x)$ and 4 (b), $y = diod(x)$ are functions for all ranges of x values.

Zardecki et al. [22] have developed a projection function from a piecewise linear function, i.e., luz(...) projection function, as shown in Equation 5.

183

Hidayat et al.

$$luz(x, a) = x + \frac{|x-a|+|x+a|}{2} \tag{5}$$

Figure 7 (a) shows the symmetric luz(...) projection function, and Figure 7 (b) shows the asymmetric luz(...) projection function. Figure 7 (a) shows the luz(...) projection function, which is symmetric about the origin. This symmetric function can be converted into an asymmetric function by shifting the function argument. The asymmetric luz(…) projection function shown in Figure 7 (b) can be viewed as a symmetric luz(…) projection function with a deflection parameter.

(a)

(b)

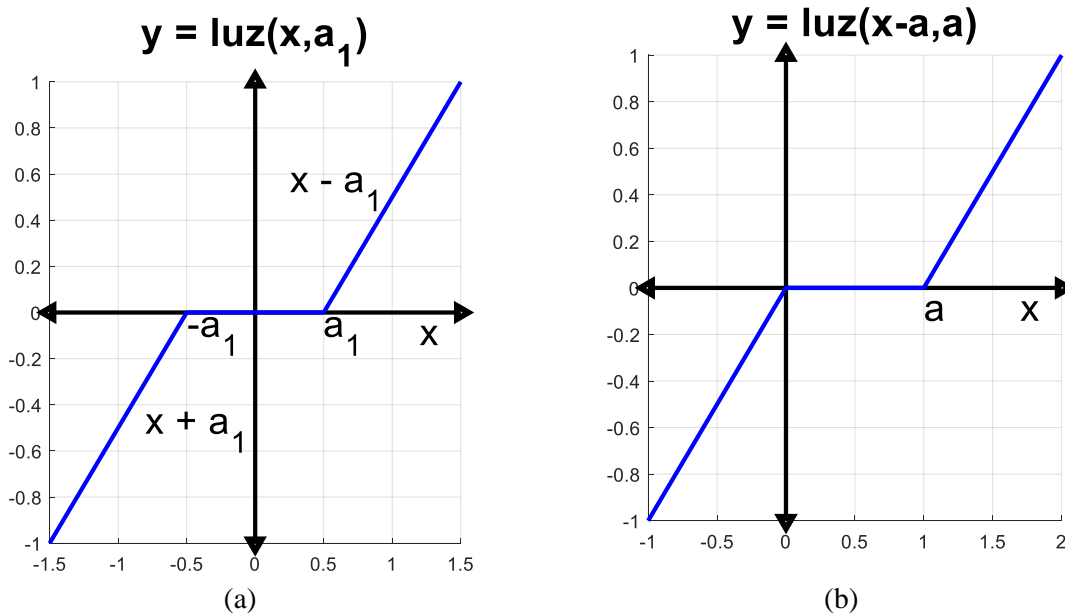**Figure 7.** Comparison of projection functions: (a) Luz(...), and (b) Asymmetric luz(...)

3.3 Model with luz(…) projection function

The luz(...) projection function in Equation 5 can be used to develop an alternative to the dense model as presented in Equation 6.

$$F_{damper} = c \cdot v - k \, luz(v, a) \tag{6}$$

The parameters c and k are the damping coefficient and the constant of the luz(...) projection function, respectively. The parameter values c, k, and a were obtained by applying the Particle Swarm Optimization (PSO) procedure using experimental data of the outer bypass MR damper with a meandering valve prototype. PSO optimization produces $c = 100,000$; $k = 8.3936$; and $a = 0.0299$. Relative Error (RE) = 0.099132 (Elapsed time is 5.560049 seconds). Figure 8 is a Matlab script for a model with the luz(...) projection function of Equation 6. The output of this Matlab script is shown in Figure 9.

```
% Parameter :                          U = Amp*cos(omega*t);
c = 10.0; k1 = 8.3936; a = 0.0299;     Vel(i) = U;
Amp = maxvel;                          f = k1*U - k2*fluz(U,a);
T = 1.9980; omega = 2*pi/T;            force88(i) = f;
nsimul = length(Force0); %             end
dt = 0.002;                            %
for i = 1 : 2000                       function luz = fluz(U,a)
t = (i-1)*dt; % deltaT;                luz = U + (abs(U-a)-abs(U+a))/2;
time(i) = t;                           end
```

Figure 8. Matlab script for the luz(...) projection function model
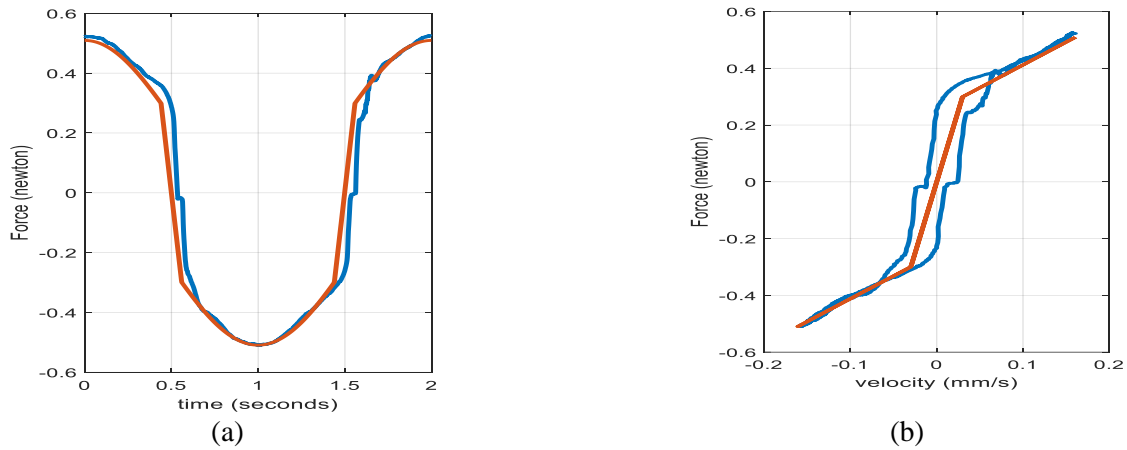
Hidayat et al.

Figure 9. Graph of damper force model with luz(...) projection function: (a) Damper force vs time; (b) Damper force vs speed.

4 Force Tracking Control

4.1 The open loop system uses a model with the luz(…) projection function

The accuracy of the MR damper model determines the accuracy of the (damper) force control system. To demonstrate this, an open loop control system was constructed to achieve the desired damping force, as shown in Figure 10. Figure 10 illustrates the damping force control block diagram. This research will compare the performance of an open loop force tracking control system using a luz(…) projection function model, the Bingham model, and the inverse Bingham model.
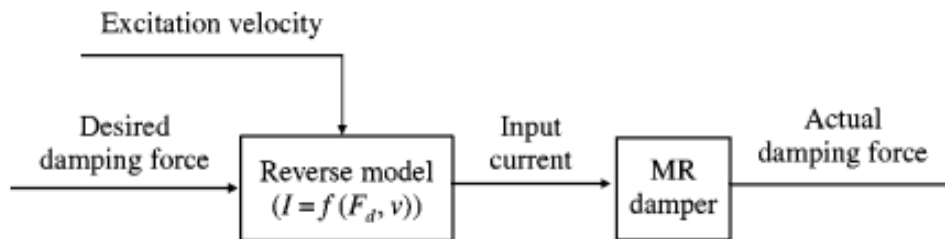

Figure 10. Block diagram of damping force control [23]

This research uses a state space approach to develop a computer simulation of an open-loop force-tracking control system. The algorithm of the simulations is as follows:

1. Determine the desired force F_d as a sinusoidal, square, sawtooth wave. Amplitude = 1, frequency = 2 rad/s.
2. Apply the Bingham inverse or inverse model of the luz(...) projection function to calculate the electric current.
3. Apply the Bingham or luz(...) projection function model to calculate the damping force.
4. The speed input for the Bingham model is $U = Fd/c$. The speed input for the model of the luz(…) projection function is $U = 1/c \int Fd \, dt$ or $U = $ cumtrapz (Fd).
5. Calculate Relative Error (RE) and similarity measure.
6. Displays the desired force and the model force.

4.2 Parameter as a function of electric current

The model parameter as a function of electric current is determined using experimental data of the outer bypass MR damper with a meandering type valve prototype using electric current varied from 0 to 1.0 amperes with intervals of 0.1 amperes. The parameter value at each current value is obtained with PSO. Next, the parameter as a function of the electric current or sensitive parameter is expressed as a linear function of the electric current input to the MR damper. The Bingham model contains parameters F_c and c_0. The parameters of F_c and c_0 as a linear function of electric current, I, are presented in Equation 7.

185

Hidayat et al.

$$F_c = 0.15859 + 0.91822 \cdot I \tag{7a}$$
$$c_0 = 1.5345 + 1.1245 \cdot I \tag{7b}$$

The R^2 values for these functions are 0.99455 and 0.85815, respectively. The model with the luz(…) projection function contains parameters c and k. Parameters c and k as linear functions of electric current, I, are given in Equation 8.

$$c = 9.4389 + 19.119 \cdot I \tag{8a}$$
$$k = 8.5275 + 14.8245 \cdot I \tag{8b}$$

The R^2 values for these functions are 0.99657 and 0.9949, respectively. This research assumes that excitation frequency and amplitude variations do not significantly influence the model output [19]. Therefore, only electric current is considered.

4.3 Inverse model

Once the desired damper force has been determined, the control input current is determined to generate the damper force of the MR damper. For the Bingham model and the model with the luz(…) projection function, the control input current is determined as shown in Figure 11.
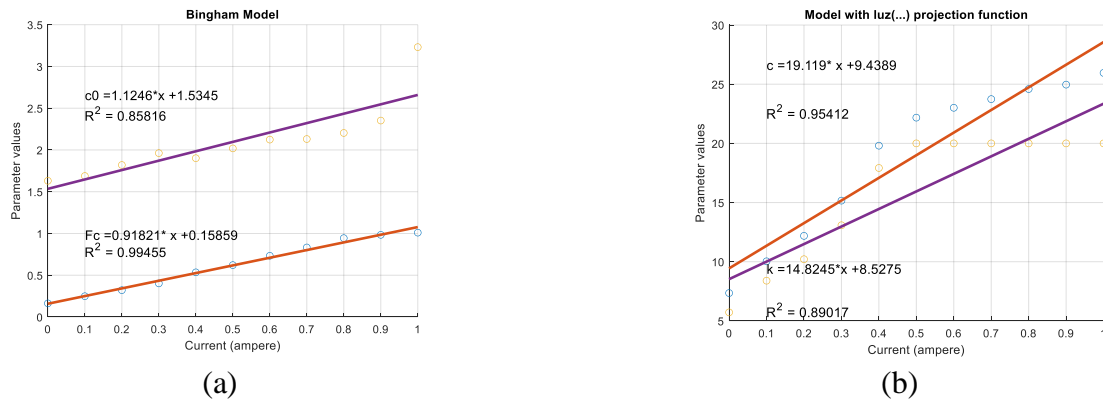

Figure 11. Parameter values as a function of current: (a) Bingham model, and (b) Model with projection function

a. Bingham inverse model

Substituting F_c and c_0 into the Bingham model Equation 1 produces the inverse Bingham model, as depicted in Equation 9.

$$F_{damper} = (0.15859 + 0,91822 \cdot I) \cdot sign(U) + (1.5345 + 1.1245 \cdot I) \cdot U + f_0 \tag{9a}$$

or

$$F_{damper} = (f_0 + 0.15859 \cdot sign(U) + 1.5345 \cdot U) + (0.91822\,sign(U) + 1.1245 \cdot U) \cdot I \tag{9b}$$

Then, electric current, I, is given in Equation 9 (c):

$$I = \frac{F_d - (f_0 + 0.1589 \cdot sign(U) + 1.5345 \cdot U)}{0.91822 \cdot sign(U) + 1.1245 \cdot U} \tag{9c}$$

where F_d is the desired damping force that will be followed.

b. Inverse model with luz(…) projection function

Parameters c and k are substituted into the model equation with the projection function luz(…) in Equation 6, producing Equation 10.

$$F_{damper} = (94389 + 19.119 \cdot I)v - (8.5275 + 14.8245 \cdot I)\text{luz}(v, a) \tag{10a}$$

or

$$F_{damper} = \big(9.4389v - 8.5275\,luz(v, a)\big) + \big(19.119v - 14.8245\,\text{luz}(v, a)\big)I \tag{10b}$$

Hidayat et al.

Then, electric current, *I,* is given in Equation 10 (c).

$$I = \frac{F_d - (9.4389v - 8.5275\ luz(v,a))}{19.119v - 14.8245\ luz(v,a)} \tag{10c}$$

where F_d is the desired damping force that will be followed.

Table 1 shows the Bingham inverse model and the inverse model of the model with the luz(…) projection function. The procedure for determining the electric current is as in research by Choi et al. [23].

Table 1. Inverse model of the Bingham model and model with projection function luz(…)

Inverse Model	
Bingham model	**Model with luz(…) projection function**
$I = \dfrac{F_d - (f_0 + 0.1589 \cdot sign(U) + 1.5345 \cdot U)}{0.91822 \cdot sign(U) + 1.1245 \cdot U}$	$I = \dfrac{F_d - (9.4389v - 8.5275\ luz(v,a))}{19.119v - 14.8245\ luz(v,a)}$

4.4 Force Tracking Control (FTC) error quantification

In this research, the performance of the MR damper model in the Force Tracking Control (FTC) scheme is evaluated in the time domain using similarity measures as in research [24]. The similarity measure is calculated in the following stages:

1. Initial data processing (data preprocessing),
2. Determine the distance function *d(A,B)*, and
3. Calculate similarity measure *s(A,B)*.

a. Data preprocessing

In the data preprocessing stage, the desired force and the force of the MR damper model are scaled using standard z-code [25], expressed in Equation 11.

$$x_i' = \frac{x_i - \bar{x}}{s} \tag{11}$$

$\bar{x}$ is the average data signal, which is calculated in Equation 12.

$$\bar{x} = \frac{1}{N}\sum_{j=1}^{N} x_j \tag{12}$$

N is the amount of data. The standard deviation *s* is calculated by Equation 13.

$$s = \sqrt{\frac{1}{N-1}\sum_{i=1}^{N}(x_i - \bar{x})^2} \tag{13}$$
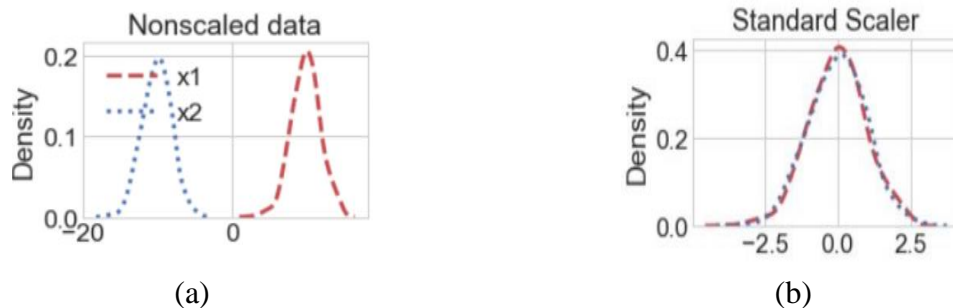

Figure 12. (a) Previous data, and (b) Data after z–code standardization is applied [25]

Equation 11 explains that the force vector *x* is translated by $\bar{x}$ and it was divided by a factor of s. This standardization technique transforms signals with a positive and negative mean so that both have the same distribution, as shown in Figure 12. Figure 12 (a) illustrates data density before z-code standardization is applied.

Hidayat et al.

b. Distance measure and similarity measure

Hamming distance measure is used to express the distance between vector A and vector B, as shown in Equation 14 [26].

$$d(A, B) = \frac{1}{N}\sum_{i=1}^{N}|A_i - B_i| \tag{14}$$

$|\cdot|$ is an absolute operator. Substituting the desired force and the simulated force (model force) into Equation 14 is obtained as Equation 15.

$$d(F^{exp}, F^{sim}) = \frac{1}{N}\sum_{i=1}^{N}|F_i^{exp} - F_i^{sim}| \tag{15}$$

The similarity measure is defined using the distance measure [26,27]. Suppose there are 2 data sets, A and B, and d is a Hamming distance measure, then the similarity measure *s(A, B)* is determined as given in Equation 16.

$$s(A, B) = 1 - d(A, A \cap B) - d(B, A \cap B) \tag{16}$$

s(A, B) is the similarity measure of data sets $A \in R^N$ and $B \in R^N$, Where N is the number of data points. A∩B is the intersection of data sets A and B, defined as Equation 17.

$$A \cap B = \min(A, B) \tag{17a}$$

where:

$$\min(A, B) = \frac{1}{2}(A + B - |A - B|) \tag{17b}$$

In this research, the similarity measure is used to measure the similarity between the damper force of the MR damper model and the desired force. The similarity measure value is in the range [0,1]. A value of 0 indicates a signal that does not coincide, and a 1 indicates a signal that does.

5 Results and Discussion

The accuracy of the MR damper force control system depends on the damper model. To demonstrate this, an open-loop force tracking control system was developed. The desired damper force is compared to the predicted one obtained from the Bingham model and the model with the luz(...) projection function, as shown in Figures 13 and 14. The desired forces are sinusoidal, square, or sawtooth signals with a constant amplitude of 1. The amplitude and frequency of the signal are constant. The results of force tracking control using the Bingham model are as follows:

1. Figure 13 (a) shows the results of force tracking control for the desired force of a sine wave with an amplitude of 1 and an angular frequency of 8 rad/s. The model's amplitude of force is greater than the desired force amplitude. This is because the Bingham model and the speed obtained from scaling the desired force are inaccurate. In addition, the force of the model does not coincide when the speed is close to 0. This is because the Bingham model does not consider the pre-yield region. RE = 0.141543 and similarity measure = 0.965255.
2. Figure 13 (b) shows the results of force tracking control for the desired force of a sawtooth wave with an amplitude of 1 and an angular frequency of 8 rad/s. The force generated by the model does not coincide with the desired force at speeds close to 0. This is because the Bingham model does not consider the pre-yield region. RE = 0.121655 and similarity measure = 0.896465.
3. Figure 13 (c) shows the results of force tracking control for the desired force of a square wave with an amplitude of 1 and angular frequency of 8 rad/s. The model force coincides with the desired force. RE = 0.0079 and similarity measure = 1.0000.

The results of force tracking control using a model with luz(...) projection function are as follows:

1. Figure 14 (a) shows the results of force tracking control for the desired force of a sinusoidal wave with an amplitude of 1 and angular frequency of 8 rad/s. The force generated by the model coincides with the desired force. RE = 0.000 and similarity measure = 1.000.

Hidayat et al.

2. Figure 14 (b) shows the results of force tracking control for the desired force of a sawtooth wave with an amplitude of 1 and a frequency of 8 rad/s. The force-generated model coincides with the desired force except when t = 0 up to 0.02 seconds. This is because the piston speed U is calculated using the integration of the desired force ($U = 1/c \int Fd\ dt$ or $U =$ cumtrapz(Fd)). RE = 0.012297 and similarity measure = 0.978109.

3. Figure 14 (c) shows the results of force tracking control for the desired force of a square wave with an amplitude of 1 and an angular frequency of 8 rad/s. The force-generated model cannot track the desired force when it changes from a negative value to a positive value, which suddenly occurs near 0, because the model with the luz(...) projection function takes into account the pre-yield region, where the speed changes from negative to positive value near 0 should not suddenly produce maximum damping force. RE = 0.056250 and similarity measure = 0.916344.

The open loop force tracking control system controls the damper using piston speed and electric current input. Compared to a closed loop force tracking control system, an open loop force tracking control system has a more straightforward instrumentation because it eliminates a force transducer, a faster response, and a minor delay phase. In addition, the open loop force tracking control system can eliminate the need to measure the MR damper piston speed.

The disturbances shown in Figure 13 can be eliminated using an open-loop force tracking control system with the luz(...) projection function model, as shown in Figure 14, especially for sinusoidal waves. Apart from the delay time at a speed of around 0, the performance of the open loop force tracking control system with the luz(…) projection function model can be considered satisfactory. A summary of the performance of the open loop force tracking control system with the Bingham model and the model with the luz(...) projection function is shown in Table 2, which shows that the model with the luz(…) projection function is superior for the sinusoidal and sawtooth of desired force. However, the Bingham model performs better for the square of desired force because of the signum function term.

Table 2. Performance of the open loop force tracking control system using the Bingham model and model with the luz(…) projection function

No.	desired force	Bingham Model		Model with luz(…) projection function	
		RE	Similarity Measure	RE	Similarity Measure
1.	Sinusoidal	0.141543	0.965255	0.000000	1.000000
2.	Sawtooth	0.121655	0.896465	0.012297	0.978109
3.	Square	0.007900	1.000000	0.056250	0.916344
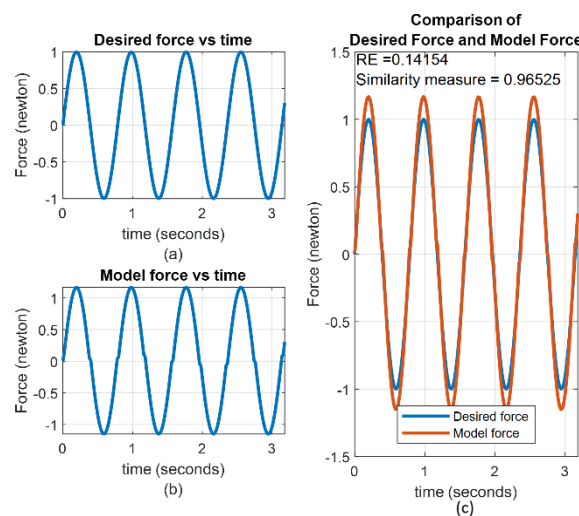
Desired force: sinusoidal
Figure 13. Force tracking using the Bingham model
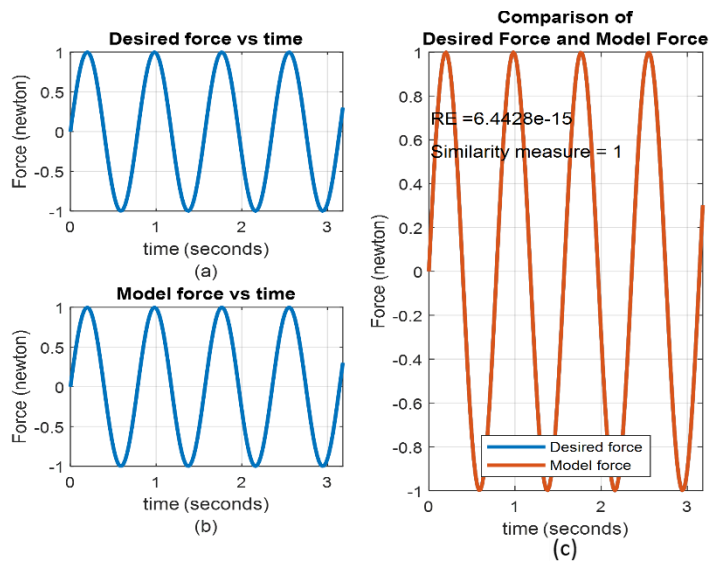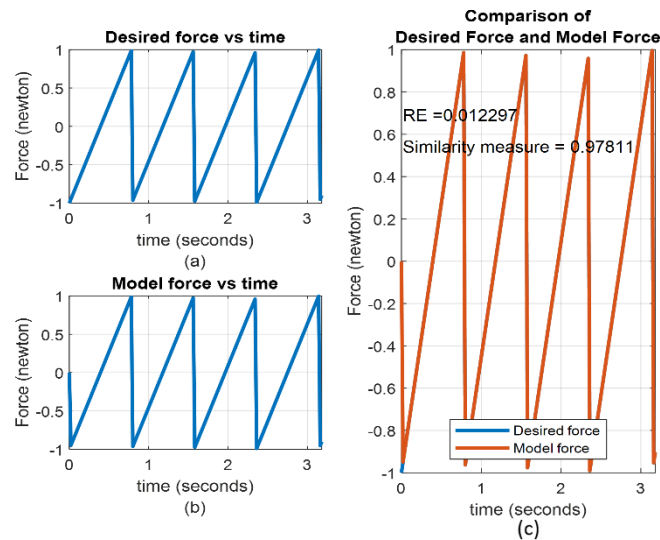
189

Hidayat et al.
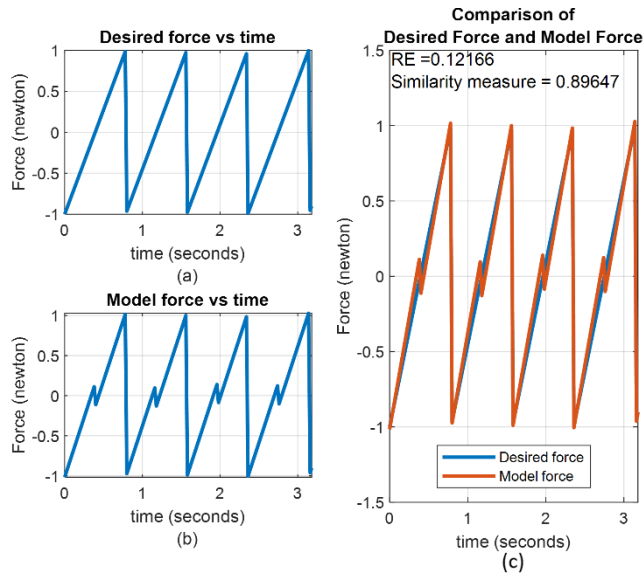
Desired force: sawtooth
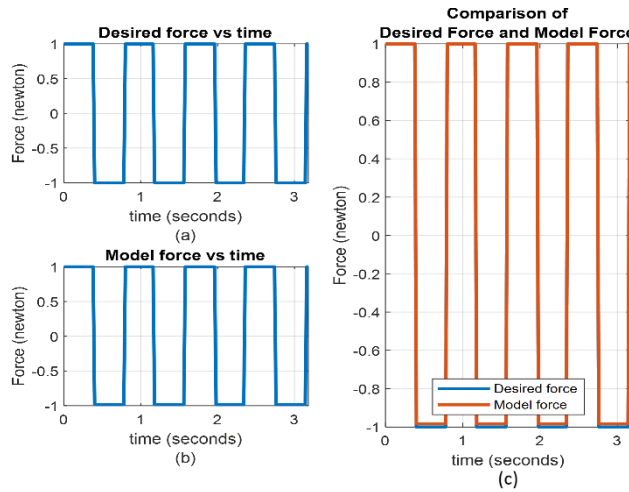
Desired force: square
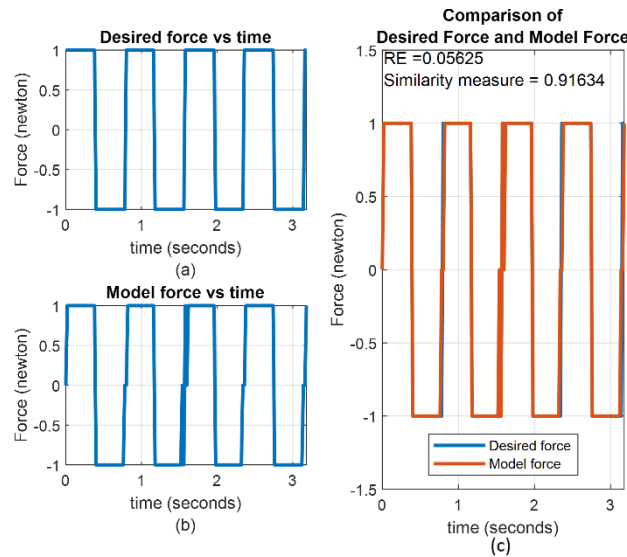
Figure 13. *Cont.*

Desired force: sinusoidal
Figure 14. Force tracking using model luz(…) projection function

Hidayat et al.

Desired force: sawtooth

Desired force: square

Figure 14. *Cont.*

6 Conclusions

This research proposes an open-loop force tracking system with a model luz(…) projection function for an outer bypass MR damper with a meandering type valve. The model parameters are determined based on the damper force data of the outer bypass MR damper with a meandering-type valve prototype obtained from experiments. The model's performance is no less accurate than the Bingham model with RE = 0.094124 compared to RE = 0.099132. However, the model luz(...) projection function considers the pre-yield region, so it can provide higher accuracy if the MR damper model is used in an open-loop force tracking control system. The conclusions from this research are:

1. The open-loop force tracking control system uses a damper model with the input of desired force and electric current. The input current is obtained from the inverse model. The inverse model uses the desired force input and MR damper piston speed.
2. The open-loop force tracking control system has simple instrumentation; it does not use a force transducer like the closed-loop force tracking control system. The open-loop force tracking control system produces a fast response.

Hidayat et al.

3. The open loop force tracking control system with the model luz(...) projection function is more accurate than the open loop force tracking control system with Bingham model for the desired force of sinusoidal and sawtooth waves with values of RE = 0.00 and similarity measure = 1.000; compared to RE = 0.1415 and similarity measure = 0.9652; and RE = 0.0123 and similarity measure = 0.978 compared to RE = 0.1216 and similarity measure = 0.8965.

4. Differences in the open-loop force tracking control system with the Bingham model can be eliminated using the open-loop force tracking control system with the luz(...) projection function model, especially for sinusoidal waves. Apart from the delay time at a speed near 0, the performance of the open loop force tracking control system with the luz(…) projection function model can be considered satisfactory.

5. This research performs computer simulations using a state space approach. The same research with Simulink/Matlab should be done immediately for comparison.

6. Speed input for the MR damper model should be improved. The following research is an open-loop system simulation using a state space approach, and speed input is determined using the Savitsky-Golay differentiation method.

References

1. C. Y. Lai and W. H. Liao, "Vibration control of a suspension system via a magnetorheological fluid damper," *J. Vib. Control*, vol. 8, no. 4, pp. 527-547, 2002.
2. Y. Li and J. Li, "Dynamic characteristics of a magnetorheological pin joint for civil structures," *Front. Mech. Eng.*, vol. 9, no. 1, pp. 15-33, 2014.
3. H. J. Jung, B. F. Spencer, Y. Q. Ni, and I. W. Lee, "State-of-the-art of semiactive control systems using MR fluid dampers in civil engineering applications," *Struct. Eng. Mech.*, vol. 17, no. 3-4, pp. 493-526, 2004.
4. S. B. Choi, Y. T. Choi, and D. W. Park, "A sliding mode control of a full-car electrorheological suspension system via hardware in-the-loop simulation," *J. Dyn. Sys. Meas. Control.*, vol. 122, no. 1, pp. 114-121, 2000.
5. F. Imaduddin, *A novel magnetorheological valve with meandering flow path structure*, Johor: Universiti Teknologi Malaysia, 2015.
6. F. Imaduddin, S. A. Mazlan, Ubaidillah, M. H. Idris, and I. Bahiuddin, "Characterization and modeling of a new magnetorheological damper with meandering type valve using neuro-fuzzy," *J. King Saud Univ. Sci.*, vol. 29, no. 4, pp. 468-477, 2017.
7. B. F. Spencer, S. J. Dyke, M. K. Sain, and J. D. Carlson, "Phenomenological Model for Magnetorheological Dampers," *J. Eng. Mech.*, vol. 123, no. 3, pp. 230-238, 1997.
8. N. M. Wereley, L. Pang, and G. M. Kamath, "Idealized hysteresis modeling of electrorheological and magnetorheological dampers," *J. Intell. Mater. Sys. Struct.*, vol. 9, no. 8, pp. 642–649, 1998.
9. D. H. Wang, and W. H. Liao, "Magnetorheological fluid dampers: A review of parametric modelling," *Smart Mater. Struct.*, vol. 20, article no. 023001, 2011.
10. D. Zardecki, "Piecewise linear luz(...) and tar(...) projections Part 1 Theoretical background," *J. Theor. Appl. Mech.*, vol. 1, no. 44 pp. 163-184, 2006.
11. D. Zardecki, "Piecewise linear luz(...) and tar(...) projections. Part 2 - Application in Modelling of dynamic system with freeplay and friction," *J. Theor. Appl. Mech.*, vol. 1, no. 44, pp. 185-202, 2006.
12. J. Rabinow, "The Magnetic Fluid Clutch," *Electr. Eng.*, vol. 67, no. 12, article no. 1167, 1948.
13. J. D. Carlson and M. R. Jolly, "MR fluid, foam and elastomer devices," *Mechatron.*, vol. 10, no. 1, pp. 555-569, 2000.
14. M. B. Cesar and R. D. Barros, "Properties and Numerical Modeling of MR Dampers," in *ICEM15: 15Th International Conference on Experimental Mechanics*, Porto, Portugal, 2012.
15. B. Ichwan, S. A. Mazlan, F. Imaduddin, T. Koga, and M. H. Idris, "Development of a modular MR valve using meandering flow path structure," *Smart Mater. Struct.*, vol. 25, no. 3, article no. 37001, 2016.
16. F. Imaduddin, S. A. Mazlan, M. A. A. Rahman, H. Zamzuri, Ubaidillah, and B. Ichwan, "A high performance magnetorheological valve with a meandering flow path," *Smart Mater. Struct.*, vol. 23, no. 6, article no. 065017, 2014.
17. F. Imaduddin, S. A. Mazlan, Ubaidillah, H. Zamzuri, and A. Y. A. Fatah, "Testing and parametric modeling of magnetorheological valve with meandering flow path," *Nonlinear Dyn.*, vol. 85, no. 1, pp. 287-302, 2016.
18. N. H. D. Nordin, A. G. A. Muthalif, M. K. M. Razali, A. Ali, and A. M. Salem, "Development and Implementation of Energy-Efficient Magnetorheological Fluid Bypass Damper for Prosthetics Limbs Using a

Hidayat et al.

Fuzzy-Logic Controller," *Inst. Electr. Electron. Eng. Access*, vol. 10, pp. 18978-18987, 2022.

19. Shimadzu, *Fatigue and Endurance Testing Systems Shimadzu Servopulser: 26*, Kyoto: Shimadzu Corp., 2014.
20. R. Stanway, J. L. Sproston, and N. G. Stevens, "Non-linear modelling of an electro-rheological vibration damper," *J. Electrost.*, vol. 20, no. 1, pp. 167-184, 1987.
21. S. Sharma, "Vibration Control in Quarter-Car Model with Magnetorheological (MR) Dampers Using Bingham Model," *J. Appl. Mech. Eng.*, vol. 7, no. 1, article no. 1000299, 2018.
22. D. Zardecki and A. Dębowski, "Non-smooth models and simulation studies of the suspension system dynamics basing on piecewise linear luz(…) and tar(…) projections," *Appl. Math. Model.*, vol. 94, pp. 619-634, 2021.
23. S. B. Choi, S. K. Lee, and Y. P. Park, "A hysteresis model for the field-dependent damping force of a magnetorheological damper," *J. Sound Vib.*, vol. 245, no. 2, pp. 375-383, 2001.
24. R. L. L. G. Hidayat, Wibowo, B. Santoso, F. Imaddudin, and Ubaidillah, "Selection of MR damper model suitable for SMC applied to semi-Active suspension system by using similarity measures," *Open Eng.*, vol. 12, no. 1, pp. 1005-1012, 2022.
25. L. B. V. D. Amorim, G. D. C. Cavalcanti, and R. M. O. Cruz, "The choice of scaling technique matters for classification performance," *Appl. Soft. Comp.*, vol. 133, article no. 109924, 2022.
26. S. Lee, and S. Shin, "Gait signal analysis with similarity measure," *Sci. World J.*, vol. 2014, article no. 136018, 2014.
27. S. Chen, B. Ma, and K. Zhang, "On the similarity metric and the distance metric," *Theory Comp. Sci.*, vol. 410, no. 24-25, pp. 2365-2376, 2009.